Published in IET Communications
Received on 11th August 2010
Revised on 21st February 2012
doi: 10.1049/iet-com.2011.0305

ISSN 1751-8628

Analytical modelling of a cognitive IEEE 802.11 wireless local area network overlaid on a cellular network

M. Moradian F. Ashtiani

Advanced Communications Research Institute (ACRI), Department of Electrical Engineering, Sharif University of Technology, Tehran, Iran
E-mail: ashtianimt@sharif.edu

Abstract: In this study, the authors propose an analytical model to evaluate the maximum stable throughput and average delay of a cognitive IEEE 802.11-based wireless local area network (WLAN) overlaid on uplink band of a cellular network. The main feature of the proposed model is to include different status of the cognitive users, that is, different spectrum opportunities for different secondary users, as the result of dynamic nature of primary users as well as different locations of the cognitive users relative to primary ones. The proposed model has been founded on an open queueing network comprised of several queueing nodes equivalent to different states of a typical secondary user. By mapping the details of MAC scheme of the cognitive WLAN and dynamic nature of spectrum opportunities onto suitable parameters of the proposed analytical model and writing the corresponding traffic equations, the authors are able to find the maximum stable throughput, that is, the maximum rate of packet generation at the cognitive nodes guaranteeing the stability of all nodes. Below this rate, that is, at the rate when all cognitive nodes are in non-saturation mode, with resort to the proposed analytical model the authors are able to evaluate the average delay comprised of the queueing delay as well as the transmission delay. The authors also show the applicability of our approach in evaluating the effect of different parameters of the cognitive network scenario, for example, the number of users, activity factors etc., onto the maximum stable throughput and non-saturation average delay. Simulation results confirm the validity of the authors analytical approach.

1 Introduction

Spectrum scarcity is one of the main concerns for the researchers and network operators. Detailed study of the spectrum shows that many parts have not been exploited efficiently [1]. Then cognitive radio technology has been developed in order to use spectrum opportunities for as much as possible. In the overlaid cognitive scenario, cognitive nodes, also called secondary nodes, sense the spectrum dedicated to licensed nodes, that is, primary nodes, find spectrum holes and transmit on those frequency bands [2]. However, cognitive nodes should be aware such that when the primary nodes become active, they free the corresponding bands. There are different network scenarios that the cognitive nodes communicate with each other, for example, *ad hoc* network [3–5], cellular network [6] etc. Many aspects of the above scenarios have been discussed in the literature. Several papers have focused on the design of routing schemes in multi-hop scenarios, for example, [7, 8]. Some have considered efficient algorithms for channel assignment at a cognitive *ad hoc* network [8]. A cross-layer approach has been used in [9] to guarantee the quality of service for real-time services in orthogonal frequency division multiplexing (OFDM)-based cognitive radio systems. Also in [10] a multilevel water-filling algorithm has been proposed, which maximises the weighted sum rate of secondary nodes in the same systems. The protocol design for spectrum mobility and handover in long term evolution (LTE) cognitive networks was addressed in [11]. On the other hand, some research works employed cognitive concepts to optimise the parameters of media access control (MAC) protocol [12].

Although many papers have focused on designing algorithms for cognitive networks, only a few have followed an analytical approach in order to evaluate them. In this respect, the authors in [6], have focused on a cellular cognitive network overlaid on a usual cellular network. There is not any difference between cognitive nodes in their transmission channel bandwidth. However, in general, owing to different locations of cognitive nodes relative to primary nodes, such an assumption is not true. The authors in [13] have considered a cognitive *ad hoc* network overlaid on a cellular network, however, the MAC scheme is a simple slotted ALOHA and the difference between channel bandwidth among cognitive nodes has not been considered. The scenario considered in [14] has combined two multiple access networks with a shared channel, a time division multiple access (TDMA)-based one for the primary nodes and a carrier sense multiple access (CSMA)-based one for the secondary nodes. Then, the authors have analysed the interaction between primary and secondary nodes when the primary nodes are not saturated. Thus, in the scenario in [14], there is not any difference among the cognitive nodes in their spectrum opportunities.

In this paper, we focus on a cognitive IEEE 802.11-based WLAN overlaid on the uplink band of a cellular network. In this scenario, with respect to a specific topology for the primary users, each cognitive node detects different number of empty channels. Thus, in general, communications among secondary nodes is done over different channel bandwidths. In such a scenario, the maximum stable throughput, that is, the maximum rate of packets received at the destinations, guaranteeing the stability of all nodes, is of crucial importance in order to evaluate the capability of the cognitive network. Another important metric is the average delay for a typical packet transmission. It is worth mentioning that different packet transmissions in the cognitive scenario may take different time durations because each packet transmission is done via different channel bandwidths. In our analysis, we propose an open queueing network [15] that represents the behaviour of a typical secondary node. By mapping the details of IEEE 802.11 distributed coordination function (DCF) MAC scheme [16], including the dynamic nature of spectrum opportunities owing to the status of primary nodes and different locations of the secondary nodes relative to primary ones, onto suitable parameters of the proposed queueing network, we are able to write traffic equations and obtain the maximum stable throughput as well as the average delay for the cognitive WLAN. Finally, we will show the effect of different parameters of the network, for example, the number of primary and secondary nodes, onto the maximum stable throughput of the cognitive network. Moreover, we verify our analytical approach by several simulations. It is worth noting that in [17], we evaluated the maximum stable throughput of a cognitive WLAN sharing the downlink band of a cellular network. Thus, in that scenario, the cognitive nodes sense the same spectrum opportunities that leads to much simplicity compared with the scenario in this paper.

Following this introduction, in Section 2, we describe the cognitive network scenario considered in this paper. We also discuss the manner of interaction between primary and secondary nodes. In Section 3, we describe our approach in analytical modelling of the cognitive network scenario. In this section, we argue how the details of the communication scenario are mapped onto the parameters of the proposed model. We also discuss how to compute the maximum stable throughput and average delay in the same section. Section 4, is dedicated to numerical results and simulations. We conclude the paper in Section 5.

2 Cognitive network scenario

In this section, we describe the assumptions for the status of primary users, secondary users, and the manner of their interactions.

2.1 Primary network model

In the considered scenario, the primary network is a typical cell of a cellular network where each cell contains N_p users. The primary users (PUs) are distributed in the cell area according to a specific spatial distribution [18]. Each user has a dedicated similar channel and there are M total channels available in the primary network ($N_p < M$). Activity of each PU is modelled independently by ON–OFF alternating states. Thus, each primary user successively switches between active and inactive states such that those states last for exponentially distributed time intervals with means T_{act} and T_{inact}, respectively, compatible with some services (e.g. voice [19, 20]). Moreover, we have focused on the uplink band of the primary network. In modern cellular networks, data services are becoming more dominant than voice services. Since the volume of data traffic in uplink is less than in downlink, focusing on uplink band appears to render more spectrum opportunities to be used by cognitive nodes. On the other hand, in downlink direction of a cellular network, all cognitive nodes are able to sense the status of primary channels similarly (neglecting misdetection errors). However, in the uplink direction, the cognitive nodes sense the primary channels differently, so it is possible that some active primary channels are sensed inactive by some cognitive nodes. In fact, the sensing state is strongly dependent on the distance between primary and secondary nodes. It is worth noting that our model can be easily changed to be used in downlink band of the primary network.

2.2 Secondary network model

The secondary (cognitive) network is an infrastructure-based WLAN comprised of an access point (AP) and a specific number of nodes. All nodes are within the transmission range of each other. AP is responsible for providing the desired service for the other secondary users (SUs). The N_s SUs in WLAN are indicated by $S_1, \ldots, S_{N_S}$. S_{N_S} is in fact the AP. Since the download traffic is usually heavier than the upload one in a WLAN, the incoming traffic at AP is much larger than those at other SUs. This leads to the first aspect of asymmetry among the SUs. However in our scenario, the incoming traffic of SUs (other than AP) that constitute the uplink traffic in secondary network are assumed to be the same. Moreover, the ratio of downlink to uplink traffic for each SU is assumed to be α ($\alpha \geq 1$).

According to random access scheme in a non-cognitive WLAN, the channel bandwidth is the same for all users. However, in cognitive WLAN, the channel bandwidth may differ for different SUs owing to different spectrum opportunities available for each of them. This is the second aspect of asymmetry among SUs which is often an inherent feature for some cognitive scenarios. In fact, the channel of a typical SU is comprised of idle primary channels sensed by the SU. In this respect, we have assumed that SUs exploit OFDM technique for their transmission, such that each idle primary channel is equivalent to a subchannel (subcarrier). Then, it is possible to use several non-contiguous primary channels in a transmission. The number of idle channels usable by an SU is dependent upon the number of PUs sensible by it as well as the activity status of them. Thus, the location of the SU and the spatial distribution of the PUs are two effective factors in constructing the transmission channel for that SU. Regarding this aspect, there should be some modifications to adapt the existing WLAN to cognitive applications. The transmission phases of a packet in the secondary network are as in the following:

1. *Contention and detection:* The communication of SUs is done based on four-way handshaking mode of IEEE 802.11 DCF in a synchronised manner [16]. Since the channel bandwidth (i.e. the number of detected idle primary channels) is not the same for all SUs, we need to specify a common channel such that all SUs can contend by sending their control signals on this channel. We assume there is a specified channel dedicated to this purpose, which is

doi: 10.1049/iet-com.2011.0305

referred to as contention channel. Thus, whenever a user has a packet, it senses the contention channel to be idle for a distributed inter frame space (DIFS). Then, the packet waits for a random number of time slots, uniformly chosen in the range of $[0, W_i - 1]$, where the window size, W_i, follows an exponential backoff procedure [16]. In the secondary network scenario, a four-way handshaking is assumed. The backoff procedure as well as request to send/clear to send (RTS/CTS) transmission is assumed to be similar to IEEE 802.11 (see [16]). If the transmission of both RTS and CTS are successful, it is followed by the packet transmission. In order to determine the channels on which the packet is transmitted, the idle primary channels should be detected by SU just before RTS is sent. The detection can be done by comparing the measured transmitted power in a primary channel with a predefined threshold. We assume perfect detection (i.e. without any misdetection). Moreover, for the sake of simplicity, a perfect power control is assumed in the primary network such that the power received at the base station, (i.e. the destination of all uplink primary transmissions), is constant. Furthermore, the propagation channel is modelled by a simple path loss. These assumptions specify a region for each SU such that only the active PUs, located in this region, are sensed busy. The PUs out of this region are sensed idle by the SU regardless of their activity status. As shown in Fig. 1, such a region is defined as the sensing region of the SU. For each SU, sensing regions are determined by transmission power of PUs, propagation channel and sensitivity of the SU's receiver.

2. *Packet transmission:* Before packet transmission starts, the secondary transmitter and receiver should negotiate about their detected idle channels. Therefore we have considered a slight change in functionality of RTS/CTS signals. In this respect, RTS contains a list of idle channels detected by the transmitter. The receiver chooses the channels from the list, which are the same as its own detected idle channels. The final list of usable channels is included in CTS signal. This list is not empty because we have assumed that a few of PUs are far enough from WLAN area such that they are not sensible by all SUs. In addition, since the channel bandwidth (comprised of idle channels sensed by both transmitter and receiver) is now known, the transmission time of the packet is also determined and inserted into CTS signal by the receiver. As a result, the other SUs will be aware of how long the packet transmission is going to last. After the pair of SUs agreed upon the channels, the transmission of packet begins. The packet is divided into parallel streams and transmitted simultaneously on agreed idle primary channels as subchannels of OFDM.

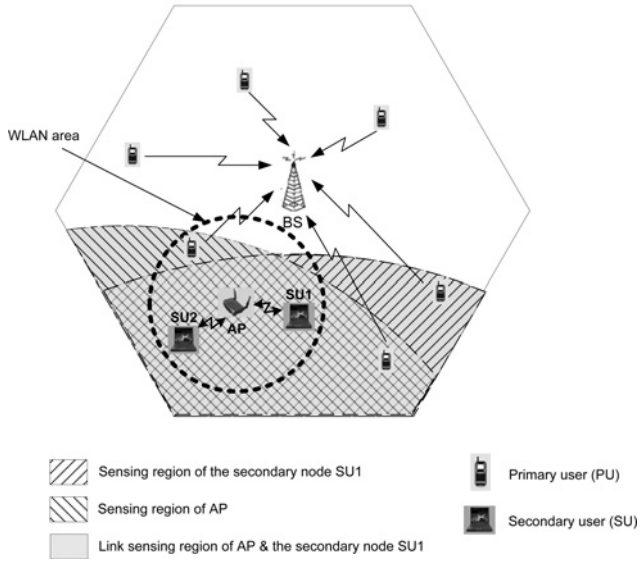

Fig. 1 *Primary and secondary network models*

2.3 Interaction between primary and secondary networks

Once a typical SU has started its transmission, the PUs that were inactive at the beginning of the transmission may change their states to active. Whenever a PU becomes active during the transmission of an SU, it interferes with that transmission. It is worth noting that only the subchannels of SU (receiver) are prone to interference which their corresponding PUs are in the sensing region of the receiver. However, the packet transmission time in a secondary link is determined by the activity status of PUs located in the sensing regions of transmitter or receiver. Thus, we mention the union of the sensing regions of AP and an SU as their link-sensing region. The link-sensing region of a typical link in secondary network has been shown in Fig. 1.

In our scenario the SU does not release a primary channel corresponding to a PU in its link-sensing region if the PU becomes active during the transmission. It is because of the fact that an SU senses the primary channels just before it starts a packet transmission. So, it cannot detect the presence of PUs during the packet transmission phases (by assuming only one transceiver for each SU). According to typical packet length in [16] and typical values of T_{act} and T_{inact} ([19, 20]), the maximum transmission time (i.e. transmission time when only one subchannel is available) of a packet is assumed to be small enough compared with T_{act} and T_{inact}. Note that the worst case for the transmission time of the packet occurs when almost all the PUs are active and also sensible by SU. The former is of very low probability. Moreover, the latter barely happens because PUs are spatially distributed across the cell and in uplink band, SUs are able to sense PUs just in their vicinity. Therefore the aforementioned assumption, which helps avoiding harmful interference for PUs, is justified by considering suitable fixed size packets.

3 Analytical modelling

In this section, we present our analytical approach for throughput and delay analysis of the secondary network. To this end, we model a typical SU (S_l) by an open queueing network [15] as depicted in Fig. 2. This network is comprised of several queueing nodes corresponding to different phases of a packet transmission. In the proposed model, the arrival of a customer to the queueing network represents the attempt to transmit a packet (including initial backoff, sending RTS etc.). The customer leaves the network after it receives its service from a subset of nodes. The model, service times and routing probabilities among the nodes are described in the following.

3.1 Model description

Our proposed model maps the different phases of the packet transmission in a typical SU (i.e. lth SU, S_l) onto the nodes of an open queueing network [15]. Different backoff stages are modelled through nodes B_i $(i = 1, \ldots, m)$ where i

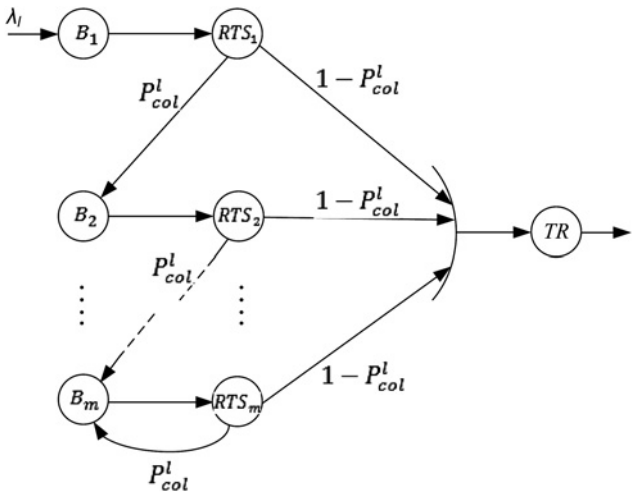

Fig. 2 *Proposed queueing network to model a typical SU*

represents the ith backoff stage. All arrived packets enter the first backoff stage (B_1). Since after the backoff time expires, immediately RTS is sent on the contention channel, the customer (i.e. the packet) is routed directly to node RTS_i after its service in node B_i ends. The node RTS_i models RTS transmission at the ith backoff stage, which in fact represents the contention phase. If the transmission of RTS is unsuccessful (with probability P_{col}^l), the packet is routed to the next backoff stage, B_{i+1}. Also, P_{col}^l denotes the collision probability of S_l caused by other SUs in the contention channel. If the contention window reaches $CW_{\max}$, which is equivalent to mth backoff stage, the packet is routed back from RTS_m to B_m. If the transmission of RTS is successful (with probability $1 - P_{\text{col}}^l$), the customer is routed from RTS_i to TR, which represents the packet transmission phase. The service time of node TR is determined according to the probability distribution of the activity status of sensible PUs, which is equivalent to different possible spectrum opportunities.

3.2 Service times and routing probabilities

In this part, service times and routing probabilities in the queueing network are discussed and calculated. These equations that are presented in the following are written for a typical SU, that is, S_l.

In nodes B_i's, since the number of backoff slots are uniformly chosen from $[0, W_i - 1]$, the average number of waiting slots is $(W_i - 1)/2$. Notice that a backoff slot may have three cases. It could be an idle time slot, frozen because of collision, or frozen owing to successful transmission. Therefore we call it a virtual time slot as in [16]. The service time in B_i is calculated as in the following

$$T_{B_i}^l = \frac{(W_i - 1)}{2} T_{vs}^l, \quad i = 1, \ldots, m \tag{1}$$

$$T_{vs}^l = P_{\text{slot}}^l T_{\text{slot}} + P_c^l T_c + P_S^l T_S^l \tag{2}$$

where $T_{B_i}^l$ and T_{vs}^l indicate the average durations of the ith backoff stage and a virtual time slot corresponding to the typical SU (S_l), respectively. P_{slot}^l, P_c^l, and P_S^l, are the probabilities of the cases in which no one transmits, more than one SU transmit and only one SU transmits at the beginning of a virtual slot of S_l, respectively. Also, T_{slot}, T_c and T_S^l are the time durations of the virtual slot in three mentioned cases, respectively, and they are derived from the following equations as in [16]

$$T_{\text{slot}} = \sigma \tag{3}$$

$$T_c = t_{\text{RTS}} + t_{\text{DIFS}} + \delta \tag{4}$$

$$T_S^l = t_{\text{RTS}} + t_{\text{DIFS}} + \delta + t_{\text{SIFS}} + \delta + t_{\text{CTS}} + \delta + T_{\text{packet}}^l + t_{\text{SIFS}} + \delta + t_{\text{ACK}} \tag{5}$$

where δ is the propagation delay and, the parameters σ, t_{RTS}, t_{CTS} and t_{ACK} stand for time durations of an idle time slot, RTS, CTS and ACK frames, respectively. Also t_{SIFS} and t_{DIFS} indicate the duration of short inter frame space (SIFS) and DIFS frames, respectively, as defined in IEEE 802.11 standard [16]. T_{packet}^l denotes the average packet transmission time corresponding to the nodes other than S_l. In order to compute P_{slot}^l, P_s^l, P_c^l and T_{packet}^l, we need to define the transmission probability of a typical SU seen by S_l. If S_l has a packet at the beginning of a slot, then its slot duration is determined based on whether other SUs transmit at that slot or not. In fact, the transmission of other nodes is significant for S_l only if it has a packet to serve. So consider observation process in which the transmission status of other nodes are observed at the beginning of non-empty slots of S_l. This leads to a set of transmission probabilities of other SUs seen by S_l, for example, $\tau_{l,k}$, denoting the transmission probability of S_k seen by S_l. Obviously, P_{slot}^l, P_s^l and P_c^l are obtained as in the following (we discuss about $\tau_{l,k}$ in the next part)

$$P_{\text{slot}}^l = \prod_{\substack{k=1 \\ k \neq 1}}^{N_s} (1 - \tau_{l,k}) \tag{6}$$

$$P_S^l = \sum_{\substack{k=1 \\ k \neq 1}}^{N_S} \prod_{\substack{k'=1 \\ k' \neq k,l}}^{N_S} \tau_{l,k}(1 - \tau_{l,k'}) \tag{7}$$

$$P_c^l = 1 - P_{\text{slot}}^l - P_S^l \tag{8}$$

Since SUs' transmission time duration are different owing to their locations relative to PUs, leading to different spectrum opportunities (i.e. different channel bandwidths), T_{packet}^l is computed as in the following

$$T_{\text{packet}}^l = \sum_{\substack{k=1 \\ k \neq l}}^{N_S} P(S_k \text{ transmits}) T_{\text{Savg}}^k \tag{9}$$

$$P(S_k \text{ transmits}) = \frac{\prod_{\substack{k'=1 \\ k' \neq k,l}}^{N_S} \tau_{l,k}(1 - \tau_{l,k'})}{P_S^l} \tag{10}$$

where T_{Savg}^k is the average packet transmission time of S_k. In (10), the successful transmission probability of S_k seen by S_l is obtained subjected to that only one SU transmits successfully. T_{Savg}^k depends on the probability distribution of the number of idle primary channels in the link-sensing region of S_k and AP, and is calculated according to the

doi: 10.1049/iet-com.2011.0305

following equations

$$T_{\text{savg}}^{k} = \sum_{j=1}^{n_k} p_j^{\text{act}} \frac{L}{C(M-j)}, \quad k = 1, \ldots, N_S - 1 \tag{11}$$

$$p_j^{\text{act}} = \binom{n_k}{j} P_a^j (1-P_a)^{n_k - j} \tag{12}$$

$$P_a = \frac{T_{\text{act}}}{T_{\text{act}} + T_{\text{inact}}} \tag{13}$$

where n_k denotes the number of PUs located in the link-sensing region of S_k and AP. L and C are the packet length of secondary users and the bit rate of a primary channel when used by an SU, respectively, and p_j^{act} is the probability that j of n_k PUs are active. P_a is the probability of a PU being active in steady state. It is worth mentioning that we have assumed the average packet length is the same for all SUs and there is not any difference between primary channels. Notice that (11) is true for all SUs except AP. On the other hand, the average packet transmission time of AP, which is denoted by $T_{\text{Savg}}^{\text{AP}}$, depends on its receiver and is derived as in the following

$$T_{\text{Savg}}^{\text{AP}} = \sum_{j=1}^{N_S-1} P(S_j \text{ is the receiver}) T_{\text{Savg}}^{\text{AP},j} \tag{14}$$

where $T_{\text{Savg}}^{\text{AP},j}$ is the average packet transmission time of AP on condition that its receiver is S_j. The average packet transmission time in a link between AP and S_j depends on the number of PUs in the link-sensing region of them and is the same for uplink and downlink transmissions. So, we can conclude that $T_{\text{Savg}}^{\text{AP},j} = T_{\text{packet}}^{j}$ derived in (9). In our scenario, the incoming packets at AP belong to one of the $N_S - 1$ SUs equally likely, so $P(S_j \text{ is receiver}) = \frac{1}{N_S - 1}$.

Finally, the service times of nodes TR and RTS_i are computed as in the following

$$T_{\text{TR}}^{l} = T_{\text{Savg}}^{l} + t_{\text{SIFS}} + \delta + t_{\text{CTS}} + \delta + t_{\text{SIFS}} + \delta + t_{\text{ACK}} \tag{15}$$

$$T_{\text{RTS}_i} = T_c = t_{\text{RTS}} + t_{\text{DIFS}} + \delta, \quad i = 1, \ldots, m \tag{16}$$

On the other hand, for routing probability in the queueing network illustrated in Fig. 2, the collision probability of S_l is derived as

$$P_{\text{col}}^{l} = 1 - \prod_{\substack{k=1 \\ k \neq l}}^{N_S} (1 - \tau_{l,k}) \tag{17}$$

where (17) states that a collision occurs if at least one of the other SUs transmits its RTS on the contention channel at the same slot which S_l is sending its RTS.

3.3 Transmission probabilities seen by a typical SU

In this part, we derive expressions for the transmission probabilities $\tau_{l,k}$ introduced in previous part. First, we obtain the transmission probability of an SU at a typical slot provided that it is non-empty. This probability equals the proportion of the number of transmission slots to the total number of non-empty slots of the SU, in steady state. Obviously this proportion does not take the duration of time slots into account. In order to compute the aforementioned proportion and remove the effect of slot durations, we interpret each slot experienced by an SU as an arrival to nodes B_i or RTS_i ($i = 1, \ldots, m$) in the queueing network corresponding to the SU. Therefore an arrival to RTS_i corresponds to a transmission slot which could be a successful or unsuccessful transmission. Moreover, an arrival to B_i implies $(W_i - 1)/2$ virtual slots in average in which the SU has not transmitted (i.e. backoff slots). If we define $\alpha_{B_i}^{k}$ and $\alpha_{\text{RTS}_i}^{k}$ as the arrival rates to nodes B_i and RTS_i in the queueing network of S_k, respectively, the transmission probability of S_k under the condition that it is non-empty, Γ_k, is calculated as

$$\Gamma_k = \frac{\sum_{i=1}^{m} \alpha_{\text{RTS}_i}^{k}}{\sum_{i=1}^{m} \frac{\alpha_{B_i}^{k}(W_i - 1)}{2} + \sum_{i=1}^{m} \alpha_{\text{RTS}_i}^{k}} \tag{18}$$

where the denominator indicates the number of all slots experienced by S_k when it is non-empty and the nominator represents the number of slots in which S_k has a transmission attempt. Considering the independent behaviour of SUs [16], the probability that S_k is being observed by S_l in transmission mode, that is, $\tau_{l,k}$, is then determined by the equation

$$\tau_{l,k} = \rho_{l,k} \Gamma_k \tag{19}$$

where $\rho_{l,k}$ is the probability that S_l observes S_k as non-empty at the beginning of a slot. This probability is not exactly the same as traffic intensity of S_k in steady state (i.e. ρ_k) because the observation instants are not completely random. Here we derive a more accurate expression for it. We have modelled the process of observation of S_k by S_l at the slots with a double-state Markov chain (Fig. 3). In this model, state '0' and state '1' represent the situations in which S_k is observed empty and non-empty by S_l at the start of a slot, respectively. If this Markov chain is solved, the steady-state probability of state '1' which is in fact $\rho_{l,k}$ is obtained as in the following

$$\rho_{l,k} = \frac{P_{01}}{P_{10} + P_{01}} \tag{20}$$

where P_{01} and P_{10} are the transition probabilities between the corresponding states (see Fig. 3). If the empty or busy status of S_k seen by S_l at the current slot is changed at the next observation slot, transition occurs between the states. We refer to the next observation slot as the next slot. However, the current and the next slots are not necessarily

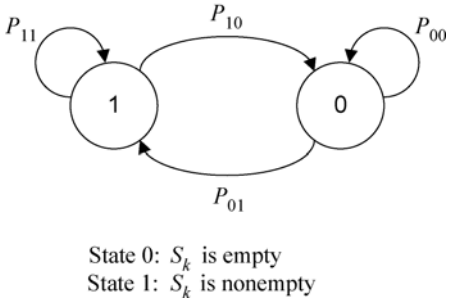

Fig. 3 *Markov chain model for the observation process of S_k seen by S_l*

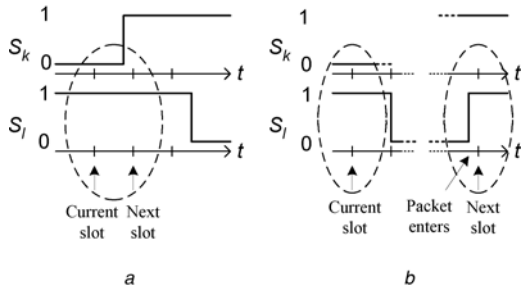

Fig. 4 *Diagrams depicting the status of next slot relative to current slot*

a S_1 is non-empty after the current slot ends
b S_1 gets empty after the current slot ends

subsequent. If the observer node, that is, S_l, does not get empty at the end of the current slot, the next slot is the subsequent one as shown in Fig. 4*a*. On the other hand, if S_l gets empty at the end of the current slot, the next slot is postponed to the slot which is coming after a packet enters the observer node as shown in Fig. 4*b*. In order to analyse P_{01} and P_{10}, the assumption of Poisson packet arrival at SUs is considered hereafter. We do the analysis in the two following steps:

1. *Analysis of* P_{01}: transition occurs from state '0' to state '1' in the two following cases:

Case 1. The current slot is a backoff, collision or successful transmission slot of S_l such that in the recent case, S_l does not get empty after the transmission. S_l remains busy at the end of a successful transmission slot with probability ρ_l, where ρ_l is the steady-state traffic intensity of S_l. This is because of the fact that the arrival of packets is assumed to be Poisson process and SUs are actually single-server nodes with arbitrary service times. In other words, we have M/G/1 nodes. According to the queueing theory, the departing packets (which are equivalent to successful transmission slots) in M/G/1 nodes (i.e. s_l), see the node busy, at the departure instants, with its steady-state probability, that is, its traffic intensity, ρ_l [21]. On the other hand, S_k is empty at the beginning of the current slot and a packet enters during the current slot. If P^l_{backoff}, P^l_{RTS}, P^l_{tx} indicate the probability of a typical slot (here the current slot) of S_l to be a backoff, collision, and successful transmission slot, respectively, and T^l_{vs}, T_c and T^l_{tx} represent their corresponding durations, the probability of *Case* 1 is written as

$$P_{\text{Case 1}} = P^l_{\text{backoff}}(1 - \mathrm{e}^{-\lambda_k T^l_{vs}}) + P^l_{\text{RTS}}(1 - \mathrm{e}^{-\lambda_k T_c}) + P^l_{tx}\rho_l(1 - \mathrm{e}^{-\lambda_k T^l_{tx}}) \tag{21}$$

$$T^l_{tx} = T_c + T^l_{\text{TR}} \tag{22}$$

where λ_k denotes the packet arrival rate at S_k. Moreover, considering the Poisson packet arrival process, the term $1 - \mathrm{e}^{-\lambda_k x}$ indicates the probability that a packet enters S_k in a slot of duration x. Also T^l_{tx} includes the durations of the contention phase, that is, T_c, derived in (4) as well as the successful transmission phase, that is, T^l_{TR}, derived in (15).

Also P^l_{backoff}, P^l_{RTS} and P^l_{tx} are calculated as in the following (similar to (18))

$$P^l_{\text{backoff}} = \frac{\sum_{i=1}^{m} \frac{\alpha^l_{B_i}(W_i-1)}{2}}{\sum_{i=1}^{m} \frac{\alpha^l_{B_i}(W_i-1)}{2} + \sum_{i=1}^{m} \alpha^l_{\text{RTS}_i}} \tag{24}$$

$$P^l_{\text{RTS}} = \frac{P^l_{\text{col}} \sum_{i=1}^{m} \alpha^l_{\text{RTS}_i}}{\sum_{i=1}^{m} \frac{\alpha^l_{B_i}(W_i-1)}{2} + \sum_{i=1}^{m} \alpha^l_{\text{RTS}_i}} \tag{25}$$

$$P^l_{tx} = \frac{(1 - P^l_{\text{col}}) \sum_{i=1}^{m} \alpha^l_{\text{RTS}_i}}{\sum_{i=1}^{m} \frac{\alpha^l_{B_i}(W_i-1)}{2} + \sum_{i=1}^{m} \alpha^l_{\text{RTS}_i}} \tag{26}$$

where (24) specifies the proportion of slots which are backoff and thus S_l does not transmit. Equations (25) and (26) indicate the probability of transmission slots being successful and unsuccessful by multiplying P^l_{col} and $1 - P^l_{\text{col}}$, respectively, by Γ_l derived in (18).

Case 2. The current slot is a successful transmission slot in which S_l gets empty at the end of the current slot with probability $1 - \rho_l$ and observes S_k non-empty at the next observation slot. Since the next slot that S_k is observed by S_l, relates to the next packet arrival time at S_l which is exponentially distributed (owing to Poisson arrivals), S_k is seen non-empty with probability ρ_k. This is due to the fact that a Poisson process observes another independent process in its steady state (PASTA [15]). The probability of Case 2 is then derived as

$$P_{\text{Case 2}} = P^l_{tx}(1 - \rho_l)\rho_k \tag{27}$$

With respect to above cases, P_{01} is finally obtained as

$$P_{01} = P_{\text{Case 1}} + P_{\text{Case 2}} \tag{28}$$

2. *Analysis of* P_{10}: transition occurs from state '1' to state '0' in the two following cases

Case 1′. The current slot is a backoff slot for S_l and a successful transmission slot for S_k, with probabilities P^l_{backoff} and P^k_{tx}, respectively. Also S_k gets empty at the end of the current slot with probability $1 - \rho_k$. The probability of this case is thus calculated as

$$P_{\text{Case 1}'} = P^l_{\text{backoff}} P^k_{tx}(1 - \rho_k) \tag{29}$$

Case 2′. The current slot is a successful transmission slot for S_l and S_l gets empty after the transmission. So the next slot of observation is exactly the next slot after the arrival of a packet at S_l. As explained before, the probabilities that S_l gets empty at the end of the current slot and observes S_k empty at the next slot are $1 - \rho_l$ and $1 - \rho_k$, respectively. Therefore the probability of this case is computed as in the following

$$P_{\text{Case 2}'} = P^l_{tx}(1 - \rho_l)(1 - \rho_k) \tag{30}$$

Finally P_{10} is computed as

$$P_{10} = P_{\text{Case 1}'} + P_{\text{Case 2}'} \tag{31}$$

3.4 Traffic equations and the maximum stable throughput

At each queueing network, traffic equations indicate the equilibrium of arrival and departure rates at each queueing node. Regarding Fig. 2, the traffic equations of the proposed queueing network corresponding to S_l are as in

doi: 10.1049/iet-com.2011.0305

the following

$$\alpha^l_{B_1} = \lambda_l \tag{32}$$

$$\alpha^l_{B_i} = P^l_{\text{col}}\alpha^l_{\text{RTS}_{i-1}}, \quad i = 2, \ldots, m-1 \tag{33}$$

$$\alpha^l_{B_m} = P^l_{\text{col}}\alpha^l_{\text{RTS}_m} + P^l_{\text{col}}\alpha^l_{\text{RTS}_{m-1}} \tag{34}$$

$$\alpha^l_{\text{RTS}_i} = \alpha^l_{B_i}, \quad i = 1, \ldots, m \tag{35}$$

$$\alpha^l_{\text{TR}} = (1 - P^l_{\text{col}})\sum_{i=1}^{m}\alpha^l_{\text{RTS}_i} \tag{36}$$

where α^l_x denotes the packet arrival rate at node x of the queueing network corresponding to S_l. Equation (34) deals with the fact that in stage m (i.e. the last backoff stage) the packets are routed back to B_m with probability P^l_{col}. By solving traffic equations, the arrival rates to the nodes of the queueing network corresponding to S_l are obtained. The traffic intensity of each node in the network is defined as its arrival rate multiplied by its average service time. In other words, single-server nodes, traffic intensity denotes the probability that the server is non-empty. So, it indicates the average number of customers at the server. Since our proposed queueing network represents the server of a typical SU, the traffic intensity of S_l is then determined by the following equation

$$\rho_l = \sum_{i=1}^{m}(\rho^l_{B_i} + \rho^l_{\text{RTS}_i}) + \rho^l_{\text{TR}} \tag{37}$$

where $\rho^l_{B_i}$, $\rho^l_{\text{RTS}_i}$ and ρ^l_{TR} are the traffic intensities for nodes B_i, RTS_i and TR in the queueing network corresponding to S_l, respectively. Equation (37) expresses that the average number of packets in the server of S_l is the summation of average number of packets in the servers of all nodes of the corresponding queueing network. Hence, by keeping (37) smaller than one, it is guaranteed that the average number of customers in the server of the SU is smaller than one which is equivalent to the stability of the SU. Among SUs, the one with largest traffic intensity is the bottleneck node, that is, it reaches the border of instability earlier than the others. Therefore the maximum stable throughput of the secondary network is the total arrival rate (i.e. $\sum_{l=1}^{N_S}\lambda_l$) which results in the traffic intensity of the bottleneck node to be on the border of instability (i.e. equal to one). According to our cognitive scenario (see Section 2), if the arrival rate at each SU is indicated by λ, then the arrival rate at AP would be $\alpha(N_S - 1)\lambda$. Then the maximum stable throughput of the secondary network (i.e. both upload and download traffic), shown by $\Lambda^{st}_{\max}$, is computed as in the following

$$\begin{aligned}\Lambda^{st}_{\max} &= \max_{\lambda}(\alpha+1)(N_S-1)\lambda|_{\rho_l\le 1, 0\le i\le N_S} \\ &= (\alpha+1)(N_S-1)\lambda_{\max}\end{aligned} \tag{38}$$

where $\lambda_{\max}$ is the maximum arrival rate at each SU other than AP leading to maximum stable throughput of the secondary network. Since in our scenario, the packet arrival rate at AP is much higher than the other SUs, AP is the node which limits the maximum stable throughput of the secondary network. In other words, this is the node which meets the instability condition earlier than the others.

3.5 Non-saturated delay analysis

In this section, we analyse the average packet delay of SUs. Since in our scenario, the packet arrival distribution at each of the single-server SUs is assumed to be Poisson and the service time has an arbitrary distribution, so each of the SUs can be modelled as an M/G/1 node. For an M/G/1 node, the Pollaczek–Khinchin formula can be used to calculate delay as in the following equation ([21])

$$D_l = E(x_l) + \lambda_l\frac{E(x_l^2)}{2(1-\rho_l)} \tag{39}$$

where D_l, $E(x_l)$ and $E(x_l^2)$ denote the average packet delay, first and the second moments of the service time corresponding to S_l, respectively. Moreover λ_l and ρ_l denote the packet arrival rate and traffic intensity of S_l, respectively. ρ_l can be derived by solving the presented equations in previous sections iteratively for a desired set of λ_j ($j = 1, \ldots, N_S$) which guarantees the stability of the network (see Section 3.4). Each packet that enters the queueing network of an SU, leaves the network after a number of probable collisions and a successful transmission. Since the collision probability of the serving packet (i.e. the packet within the transmission process) at the queueing network corresponding to S_l is considered to be P^l_{col}, then the $E(x_l)$ and $E(x_l^2)$ are calculated according to the following equations

$$E(x_l) = \sum_{k=1}^{\infty}(P^l_{\text{col}})^{k-1}(1 - P^l_{\text{col}})\overline{x_{l,k}} \tag{40}$$

$$E(x_{l^2}) = \sum_{k=1}^{\infty}(P^l_{\text{col}})^{k-1}(1 - P^l_{\text{col}})\overline{x^2_{l,k}} \tag{41}$$

where $\overline{x_{l,k}}$ denotes the average packet service time corresponding to S_l, on condition that the kth transmission of the packet is successful, that is, $k-1$ collisions have occurred. Thus, $\overline{x_{l,k}}$ can be derived from the following equations:

$$x_{l,k} = \begin{cases} \sum_{j=1}^{k}(T^l_{B_j} + T_{\text{RTS}_j}) + T^l_{\text{TR}}; & 1 \le k \le m \\ \sum_{j=1}^{m}(T^l_{B_j} + T_{\text{RTS}_j}) & \\ \quad +(k-m)(T^l_{B_j} + T_{\text{RTS}_j}) + T^l_{\text{TR}}; & m \le k \end{cases} \tag{42}$$

where $T^l_{B_j}$, T_{RTS_j}, and T^l_{TR} indicate the service times of nodes B_j, RTS_j, and TR of the queueing network corresponding to S_l. By inserting (40)–(42) in (39), we are able to compute the average delay for a typical packet of the corresponding wireless node, S_l.

4 Numerical and simulation results

In this section, we present some numerical results in order to evaluate the maximum stable throughput and average delay of a cognitive WLAN in different conditions. We also present the simulation results in order to validate the accuracy of our model. The simulation has been done in MATLAB environment. The values of different parameters in analysis and simulation have been listed in Table 1 ([16], [20]). Moreover, α (see Section 2.2) is assumed to be one which

Table 1 Typical values of parameters in simulation and analysis

parameter	Numerical value
M	50
T_{act}	0.3 s
T_{inact}	0.5 s
L	8000 bit
C	200 kbps
T_c	300 μs
T_{slot}	50 μs
N_p	40
N_s	21

corresponds to a symmetric service, for example, VoIP (Voice over IP) service [22].

Without loss of generality, we have applied a specific spatial topology for PUs in our simulation and analysis. We have placed PUs in different regions in the cell such that 50% of them are sensible by all SUs and 20% are out of the sensing region of them. Thus, for each packet transmission in the cognitive network, 20% of the primary channels are available irrespective of the corresponding PUs' status. On the other hand, 50% of the primary channels are sensed similarly by all SUs, however, the usability of the remaining 30% of the channels depends on the location of the SU. Hence, the performance metrics (throughput and delay) are dependent upon the spatial topology of the wireless nodes. By having the spatial distribution of PUs, the maximum stable throughput of the cognitive WLAN could be obtained in a more general case. In our analyses, we have focused on a specific spatial topology with the aforementioned proportions in different regions, as typical values.

In Fig. 5 the effect of spatial distribution of PUs on the maximum stable throughput of secondary network has been studied. To this end, we have changed the percentage of PUs which is sensible by all SUs. As shown in Fig. 5, the maximum stable throughput decreases nearly linear as the percentage of PUs in the sensing region of WLAN (i.e. all SUs) increases.

The influence of activity factor of PUs on the maximum stable throughput of secondary network is depicted in Fig. 6. The activity factor is a characteristic of the service type provided by the primary network. Increasing the activity factor decreases the spectrum opportunities for SUs

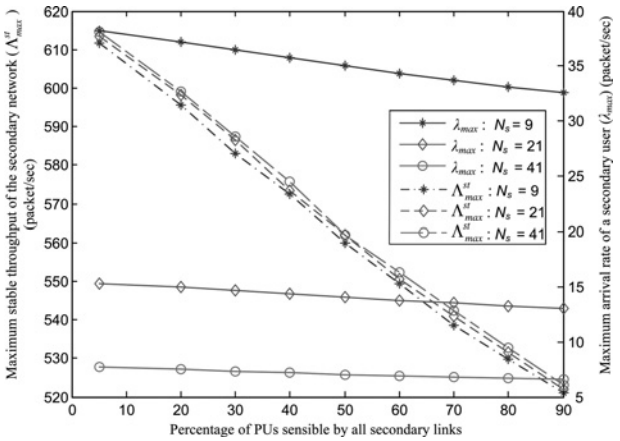

Fig. 5 *Effect of spatial distribution of PUs on the maximum stable throughput of the secondary network*

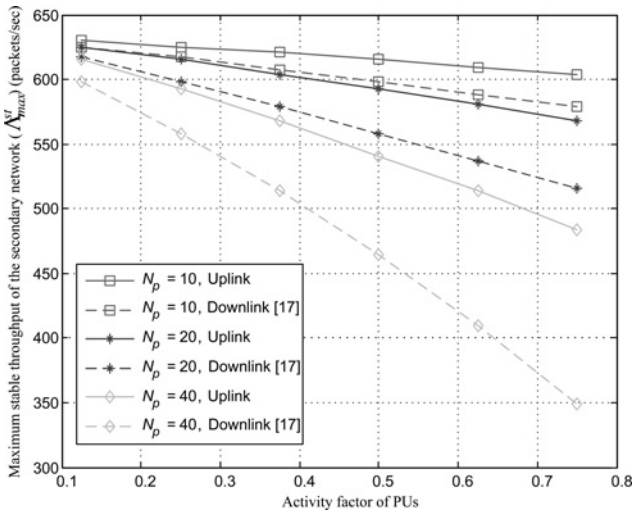

Fig. 6 *Effect of activity factor on the maximum stable throughput of the secondary network*

leading to a degradation in the maximum stable throughput of secondary network. As shown in Fig. 6, for larger number of PUs, the increment of the activity factor causes more degradation in the maximum stable throughput. This is due to the fact that in larger number of PUs, the number of sensible PUs by all SUs also increases, so the activity of PUs more strongly affects the spectrum opportunities (assuming that the spatial distribution of PUs does not change). Also the results where the secondary network utilises the downlink band of the primary network [17] have been illustrated in Fig. 6. As shown in Fig. 6, at

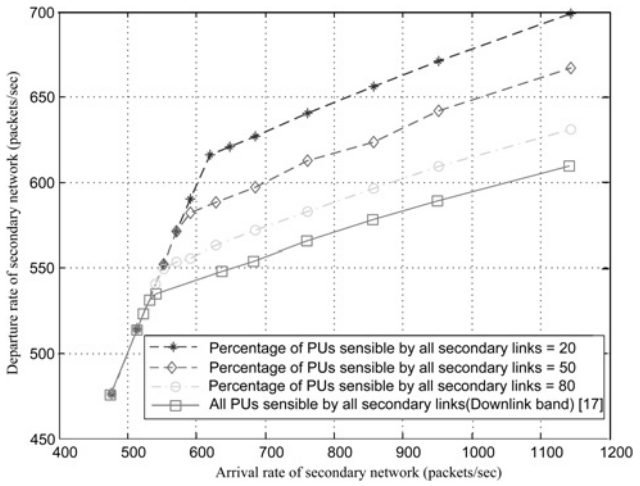

Fig. 7 *Simulation results for departure rate against arrival rate in the secondary network*

Table 2 Ratio of departure rate to arrival rate at AP for three types of arrivals

Arrival rate at AP (λ)	Poisson	Uniform	MMPP $\lambda_1 = 2\lambda$, $\lambda_2 = 0.5\lambda$
266.66	1	1	1
271.42	1	1	0.994
276.19	1	1	0.960
285.71	1	1	0.918
290.47	0.995	0.994	0.885
295.23	0.969	0.969	0.850

doi: 10.1049/iet-com.2011.0305

Table 3 Simulation results for average delay corresponding to three types of arrivals with different rates but nearly the same traffic intensities

Poisson		Uniform		MMPP	
Traffic intensity of AP	Average delay(s)	Traffic intensity of AP	Average delay(s)	Traffic intensity of AP	Average delay(s)
0.30	0.0034	0.29	0.0029	0.29	0.0131
0.40	0.0040	0.38	0.0033	0.37	0.0150
0.48	0.0047	0.44	0.0036	0.46	0.0208
0.60	0.0065	0.56	0.0046	0.56	0.0313

activity factor of 0.4, the increase in maximum stable throughput of the secondary network amounts to 1.5, 4.2 and 10.3% for 10, 20 and 40 PUs, respectively. This increase is due to the fact that in uplink band, SUs can take advantage of active primary channels that their corresponding PUs are far away to be sensed by SUs, without causing any problem to them. As the number and activity factor of PUs get larger, spatial opportunities play more vital role in enhancing the maximum stable throughput of the secondary network.

In order to confirm our modelling approach, we have plotted the simulation results in which the throughput (i.e. the departure rate of packets) is measured for different arrival rates. To this end, the simulation is carried out for three types of arrival processes. Moreover, we have simulated the MAC scheme of IEEE 802.11, discussed in Section 2, for each packet transmission. In our simulation, the physical effects have been ignored and the packets play the role of information entities. Then, we have counted the number of generated packets as well as the number of packets received successfully in a large time interval (equivalent to a large number of generated packets in order of hundred thousand ones). By dividing the counted number of packets into the time interval, we obtain the arrival and departure rates. In order to be certain about the validity of our results, we have considered the simulation for two different sufficiently large time intervals such that the results are within 0.5% difference. As shown in Fig. 7, because of stability, at the rates below the maximum stable throughput, the arrival rate equals the departure rate. However, for arrival rates greater than the maximum stable throughput, some packets incur infinite delay. In this case the departure rates of the saturated nodes do not increase anymore. Notice that since the SUs (other than AP) have the same arrival rate in our scenario, the above discussion holds true for AP which is the throughput limiting node. In fact, after the arrival rate exceeds the rate corresponding to the maximum stable throughput (i.e. λ_{max}), the departure rate of AP does not increase, however the other SUs are still capable of supporting higher rates. For this reason the plot in Fig. 7 has a slight increasing slope. Actually the knee of the simulation curve shows the maximum stable throughput. Comparing the knees of the curves with the analytical results in Fig. 5 shows a nearly 3% difference. The results for the downlink scenario are also depicted in Fig. 7. As shown in Fig. 7, the maximum stable throughput of the secondary network in downlink band is less than the uplink one owing to lack of spatial opportunities.

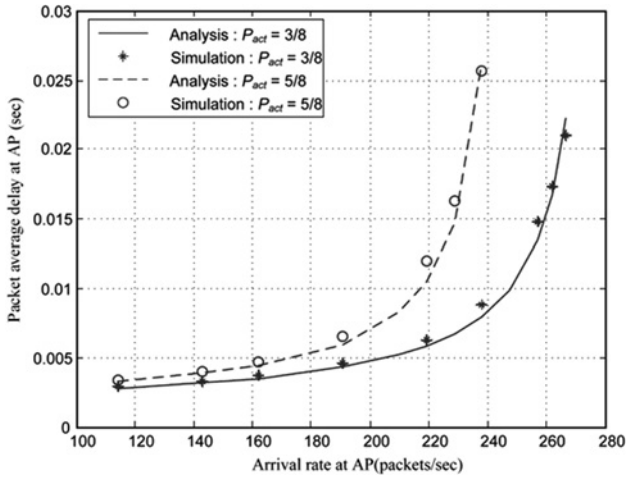

Fig. 8 *Analytical and simulation results for average delay corresponding to the packet transmissions by AP*

In order to show the capability of our model in evaluating the average delay we have plotted it for rates lower than the maximum stable throughout (i.e. non-saturation mode) and compared the results with simulation in Fig. 8. The results have been plotted for two activity factors. As we observe the analytical results are in close match with simulation results. The small amount of difference mainly reverts to a bit difference between traffic intensities (ρ) at simulation and analysis (corresponding to aforementioned mismatch in maximum stable throughput). In fact, $1-\rho$ appears in the denominator of (39), leading to more mismatch in delay for a small mismatch in ρ.

As we indicated, our analytical approach exploits the nature of Poisson process for the arrivals (e.g. Section 3.3). In order to illustrate the difference between the results of our analytical approach based on Poisson process with the simulation results based on some other arrival processes, we have considered Markov modulated Poisson process (MMPP) and arrivals with uniform inter-arrival times.

In the former case, we have considered two states with average sojourn times T_1, T_2, corresponding to Poisson processes with rates λ_1, λ_2, respectively ($T_1 = 0.05$ s, $T_2 = 0.2$ s). Table 2 shows that there is not any significant change in the maximum stable throughput for the non-Poisson arrival processes, compared with Poisson arrival process with the same rate. However, the story of average delay is different. In fact, in evaluating the average delay, the results for three types of arrivals with the same rate are much different. In order to have a relatively fair comparison we have selected the arrival rates such that the traffic intensities for three types of arrivals are nearly the same. As we observe in Table 3, the results of arrival process with uniform inter-arrival time is very near to the case of Poisson process, however, the delays for MMPP are much larger. This is due to the fact that according to our model for MMPP, in some time intervals (corresponding to first state of MMPP) the temporary arrival rate is two times of the steady-state arrival rate, leading to some packet

accumulation. They should bear larger delay. So, the average delay is larger than the case of Poisson arrival.

5 Conclusions

In this paper we presented an analytical model for a cognitive IEEE 802.11-based WLAN overlaid on a cellular network. We mapped the details of the corresponding MAC protocol as well as different spectrum opportunities owing to spatial traffic distribution of PUs, onto suitable parameters of an open queueing network. Our model included both aspects of asymmetry in traffic arrival rates at different SUs as well as different spectrum opportunities corresponding to SUs. In order to obtain the parameters of the proposed queueing network, we needed the observed transmission probability of a typical SU by other SUs. By modelling the observation process with a double-state Markov chain, we computed the corresponding probabilities. Finally, through solving the traffic equations of the proposed queueing network, we were able to attain traffic intensities of SUs in different arrival rates which leaded us to the maximum stable throughput of the secondary network. We applied our analytical approach for different set of parameters and showed their effects onto the maximum stable throughput of the cognitive WLAN. Furthermore, we plotted the non-saturation average delay for different arrival rates. We also showed if Poisson arrival process is replaced by an MMPP or an arrival process with uniform inter-arrival time the maximum stable throughput remains nearly unchanged but the average delay for MMPP is very different. Finally, we validated our analytical approach by several simulations.

6 Acknowledgment

This research work has been partially supported by Iran Telecom Research Centre (ITRC) under grant no. 500.19167 and Iran National Science Foundation (INSF) under grant no. 88114.46-2010.

7 References

1 Federal Communications Commission (FCC), *Spectrum Policy Task Force*, November 15, 2002. ET Docket no. 02-135
2 Haykin, S.: 'Cognitive radio: brain-empowered wireless comm.', *IEEE J. Sel. Areas Commun.*, 2005, **23**, (2), pp. 201–220
3 Zhao, L., Tong, A.S., Chen, Y.: 'Decentralized cognitive MAC for opportunistic spectrum access in ad hoc networks: a POMDP framework', *IEEE J. Sel. Areas Commun.*, 2007, **25**, (3), pp. 589–599
4 Hsu, A., Wei, S., Kuo, C.: 'A cognitive MAC protocol using statistical channel allocation for wireless ad-hoc networks'. Proc. WCNC, 2007, pp. 105–110
5 Wang, L., Chen, A., Wei, D.: 'A cognitive MAC protocol for QoS provisioning in overlaying ad hoc networks'. Proc. CCNC, 2007, pp. 1139–1143
6 Tang, S., Mark, B.L.: 'Modeling and analysis of opportunistic spectrum sharing with unreliable spectrum sensing', *IEEE Trans. Wirel. Commun.*, 2009, **8**, (6), pp. 3142–3150
7 Cheng, G., Liu, W., Cheng, W.: 'Joint on-demand routing and spectrum assignment in cognitive radio networks'. Proc. ICC'07, 2007, pp. 6499–6503
8 Shiang, H.-P., Schaar, M.V.D.: 'Distributed resource management in multihop cognitive radio networks for delay-sensitive transmission', *IEEE Trans. Veh. Technol.*, 2009, **58**, (2), pp. 941–953
9 Zhang, Y., Leung, C.: 'Cross-layer resource allocation for real-time services in OFDM-based cognitive radio systems', *Telecommun. Syst.*, 2009, **42**, (1–2), pp. 97–108
10 Tang, Z., Wei, G., Zhu, Y.: 'Weighted sum rate maximization for OFDM-based cognitive radio systems', *Telecommun. Syst.*, 2009, **42**, (1–2), pp. 77–84
11 Chen, Y., Cho, C., You, I., Chao, H.: 'A cross-layer protocol of spectrum mobility and handover in cognitive LTE networks'. Proc. Simulation Modeling Practice and Theory, 2011, pp. 1723–1744
12 Deng, D., Chen, H.C., Chao, H.C., Huang, Y.M.: 'A Collision alleviation scheme for IEEE 802.11p VANETS', *Wirel. Pers. Commun.*, 2011, **56**, (3), pp. 371–383
13 Feizi-Khankandi, S., Ashtiani, F.: 'Lower and upper bounds for throughput capacity of a cognitive ad hoc network overlaid on a cellular network'. Proc. WCNC, 2008, pp. 2759–2764
14 Li, H., Grace, D., Mitchell, P.D.: 'Throughput analysis of non-persistent carrier sense multiple access combined with time division multiple access and its implication for cognitive radio', *IET Commun.*, 2010, **4**, (11), pp. 1356–1363
15 Chio, X., Miyazawa, M., Pinedo, M.: 'Queueing networks' (John Wiley & Sons, 1999)
16 Bianchi, G.: 'Performance analysis of the IEEE 802.11 distributed coordination function', *IEEE J. Sel. Areas Commun.*, 2000, **18**, (3), pp. 535–547
17 Moradian, M., Ashtiani, F.: 'Throughput analysis of cognitive IEEE 802.11 WLAN sharing the downlink band of a cellular network'. Proc. IEEE ICC'11, Kyoto, June 2011
18 Ashtiani, F., Salehi, J.A., Aref, M.R.: 'Mobility modeling and analytical solution for spatial traffic distribution for wireless multimedia wireless networks', *IEEE J. Sel. Areas Commun.*, 2003, **21**, (10), pp. 1699–1709
19 Das, K., Morgera, S.D.: 'Interference and SIR in integrated voice/data wireless DS-CDMA networks-a simulation study', *IEEE J. Sel. Areas Commun.*, 1997, **15**, (8)
20 Yeh, W.P., Hammond, J.L., Tipper, D.: 'Sensitivity of bandwidth allocation algorithms for unidirectional networks to voice parameters'. Proc. IEEE ICC'90, April 1990, pp. 1295–1299
21 Kleinrock, L.: 'Queueing systems'. vols. I, II (John Wiley & Sons, 1975)
22 Cai, L.X., Shen, X., Mark, J.W., Xiao, Y.: 'Voice capacity analysis of WLAN with unbalanced traffic', *IEEE Trans. Veh. Tech.*, 2006, **55**, (3), pp. 752–761

doi: 10.1049/iet-com.2011.0305